Spectroscopic Identification of the Lithium Ion Transporting Species in LiTFSI-Doped Ionic Liquids

Jean-Claude Lassègues,*,† Joseph Grondin,† Christian Aupetit,† and Patrik Johansson‡

ISM, UMR 5255, CNRS, Université Bordeaux I, 351 Cours de la Libération, 33405 Talence Cedex, France, and Department of Applied Physics, Chalmers University of Technology, SE-41296 Göteborg, Sweden

Received: July 11, 2008; Revised Manuscript Received: October 6, 2008

The solvation of the lithium ion in LiTFSI-doped ionic liquids based on alkyl-substituted imidazolium cations and bis(trifluoromethanesulfonyl)imide anions ($TFSI^-$) was investigated by infrared and Raman spectroscopies. The spectral changes occurring for some $TFSI^-$ vibrations sensitive to the lithium coordination were analyzed with the help of DFT calculations. In addition, the vibrations of the lithium ion in its solvating cage were found to produce a broad IR absorption band centered at 374 cm^{-1}. For low to moderate LiTFSI mole fractions, $0.08 < x < 0.2$, the $[Li(TFSI)_2]^-$ solvating cage was found to involve bidentate coordinations of Li^+ with two oxygen atoms of one anion in the trans (C_2) conformation and two oxygen atoms of the other anion in the cis (C_1) conformation. At higher LiTFSI concentration, up to $x = 0.5$, the lithium ion−TFSI coordination number progressively becomes less than 2, indicating the possible formation of aggregates.

Introduction

A new class of liquid electrolytes for lithium batteries has been in development for a few years.[1−14] Such electrolytes are obtained by doping an ionic liquid (IL), composed, for example, of alkyl-substituted imidazolium or pyrrolidinium cations and bis(trifluoromethanesulfonyl)imide anions ($TFSI^-$), by the lithium salt LiTFSI. The doping levels are usually limited to a domain where the mixture remains liquid at room temperature, i.e., to typical LiTFSI mole fractions of $x \leq 0.4$. For practical applications, a compromise has to be found between the increase in the lithium charge carrier concentration and the concomitant increase in the viscosity and resistivity. Many properties such as electrochemical and chemical stabilities, lithium transference number, safety, and environmental compatibility, must also be investigated and optimized.

From a fundamental point of view, the lithium ion solvation process is important to understand, because it is related to the conductivity and lithium transport number, i.e., to properties of the electrolyte that are known to affect strongly the performances of lithium batteries. The theoretical and experimental studies performed to date indicate that Li^+ coordinates preferentially to the oxygen atoms of the SO_2 groups held by the $TFSI^-$ anion $N(CF_3SO_2)_2^-$. The number and structure of the surrounding anions are more difficult to determine.

According to recent studies using Raman spectroscopy and DFT calculations, $[Li(TFSI)_2]^-$ complexes are formed by two bidentate Li···O coordinations for lithium mole fractions smaller than ∼0.2.[5,10,13] The diffusion coefficients of the ^1H, ^7Li, and ^{19}F nuclei measured by NMR spectroscopy are interpreted in terms of $[Li(TFSI)_n]^{(n-1)-}$ solvates with $n = 2$,[13] 3,[9] or 4.[14] Molecular dynamics (MD) calculations predict $[Li(TFSI)_n]^{(n-1)-}$ solvates with $n = 3$ or 4,[4,12] but Borodin et al. also developed an interesting analysis of the Li^+ environment as a function of the lithium concentration.[4] According to these authors, in addition to $[Li(TFSI)_n]^{(n-1)-}$ solvates, significant lithium aggregation would occur through formation of $Li^+\cdots(Li^+\cdots Li^+)_n$ clusters with $Li^+\cdots Li^+$ distances of less than 5 Å, each lithium being connected to its neighbor through the O═S═O part of the $TFSI^-$ anions. A direct illustration of this kind of arrangement is provided by the structure of the $Li_2(EMI)(TFSI)_3$ compound in which the two crystallographically independent lithium ions are trigonal-bipyramidally coordinated by five oxygens to form a two-dimensional network.[6] Aggregates of the $Li^+\cdots(Li^+\cdots Li^+)_n$ kind have also been encountered in crystalline complexes of lithium salts with poly(ethylene oxide) oligomers.[15,16] For instance, the $(G4)_1$,LiX complexes, where G4 is tetraglyme, consist of double-helix dimers in which two six-coordinated Li^+ cations are coordinated by two G4 molecules, the $Li^+\cdots Li^+$ distance being less than 5 Å.[15] In $P(EO)_6$:LiX complexes, two PEO chains wrap around the cations coordinated to three oxygen atoms of one chain and two oxygen atoms of the other. There are two typical $Li^+\cdots Li^+$ distances along the chain axis of about 6.5−7.5 and 4.5−5.5 Å.[16] To the best of our knowledge, there is at present no spectroscopic evidence of $Li^+\cdots(Li^+\cdots Li^+)_n$ aggregates in LiTFSI-doped ILs.

This short summary shows that the structure of the Li^+ solvation shell in LiTFSI-doped ILs is complex and not fully elucidated. In this context, the aim of the present work was to critically investigate the potentialities of vibrational spectroscopy. To the best of our knowledge, three different LiTFSI-doped ILs involving alkyl-substituted imidazolium cations have previously been investigated by Raman spectroscopy (Table 1).[5,10,12,13] We gathered the results obtained for these systems and tried to rationalize the available data, in particular for the prediction of the lithium solvation number. The limits and possibilities of this approach together with the complementarity of IR spectroscopy and DFT calculations are emphasized.

Experimental Methods

The ILs used and described in Table 1 were purchased from Solvionics (>99% purity). The LiTFSI salt (>99.95%) was obtained from Aldrich. These products were not further purified and were always kept in a glovebox under argon (1 ppm H_2O

* Corresponding author. E-mail: jc.lassegues@ism.u-bordeaux1.fr.
† ISM.
‡ Chalmers University of Technology.

10.1021/jp806124w CCC: $40.75
Published on Web 12/11/2008

TABLE 1: Ionic Liquids Based on Alkyl-Substituted Imidazolium and Lithium Salts of $TFSI^-$ Investigated by Raman Spectroscopy[a]

	$(1-x)$EMITFSI,xLiTFSI EMI^+ = 1-ethyl-3-methyl imidazolium	$(1-x)$BMITFSI,xLiTFSI BMI^+ = 1-butyl-3-methyl imidazolium	$(1-x)$BMMITFSI,xLiTFSI $BMMI^+$ = 1-butyl-2,3-di methylimidazolium
investigated mole fractions	$x = 0.125$ (ref 7) $0 < x < 0.5$ (this work) $0 < x < 0.15$ (ref 10)	$0 < x < 0.4$ (ref 13)	$0 < x < 0.38$ (ref 12) $0 < x < 0.5$ (this work)
density	$1.52 + 0.2263x + 0.1243x^2$	$1.43 + 0.2381x + 0.1598x^2$	$1.42 + 0.2452x + 0.1813x^2$
C_T	$3.8198 + 2.09333x$	$3.3296 + 2.2368x$	$3.1872 + 2.3278x$

[a] Densities were derived from the volume parameters of ref 8. x is the LiTFSI mole fraction, and C_T is the total molarity of the $TFSI^-$ anions. The molarities of the lithium and imidazolium cations are xC_T and $(1-x)C_T$, respectively. The densities and molarities are parametrized for $0 < x < 0.4$. All data obtained at room temperature.

and O_2). The entire sampling procedure for the IR and Raman experiments, unless otherwise indicated, was performed inside the glovebox. The mixtures with LiTFSI were prepared by weighing the components, which gives accurate values of the LiTFSI mole fraction, x. However, because the Raman intensity and the IR absorbance are proportional to the number of molecules per unit volume, the relevant concentration unit for quantitative measurements is molarity. Densities, needed to convert mole fractions to molarities, are not always available. Ye and Shreeve derived volume parameters from which these densities, and hence the molarities, can be predicted,[8] as was successfully tested by Monteiro et al. on the $(1-x)$BMMITFSI,xLiTFSI system.[12] Parametrized expressions of the density and total anion concentration, C_T, as a function of x are reported in Table 1 for the three investigated systems. It is then easy to deduce the molarities of the lithium ions, xC_T, and of the imidazolium ions, $(1-x)C_T$, for any x value in the range $0 < x < 0.4$.

After the samples had been introduced into sealed glass tubes, the Raman spectra were recorded as previously described.[5,13] The spectra were normalized by integrating the intensity of the most intense Raman band between 775 and 717 cm^{-1}. To record the IR spectra, two methods were used. Liquid films were first prepared between cesium iodide windows. The very strong anion absorptions situated in the 1100−1300 cm^{-1} region need film thicknesses of less than 0.5 μm that are difficult to achieve. The much less intense absorptions situated in the far-IR region are easier to observe using thicker films. The spectra down to 200 cm^{-1} were recorded with a Bruker 113v spectrometer. The mid-IR spectra down to 600 cm^{-1} were more conveniently recorded using a single-reflection diamond attenuated total reflection (ATR) system (Specac) with a refractive index of $n_1 = 2.4175$ installed on a Nicolet Nexus spectrometer. The ATR spectra were not corrected for the variation of the penetration depth, $d_p = \lambda/\{2\pi n_1[\sin^2\Theta_i - (n_2/n_1)^2]^{1/2}\}$, as a function of the wavelength, λ, and of the refractive index of the solution, n_2, as no quantitative measurement were made using the IR data. Note, however, that, for a typical absorption band extending over a few tens of wavenumbers, the wavelength correction is negligibly small, whereas the refractive index correction, although more important, remains moderate. Indeed, the n_2 value for the $(1-x)$EMITFSI,xLiTFSI system at 295 K was found to decrease from 1.4225 at $x = 0$ to 1.4215, 1.4185, and 1.4155 at $x = 0.1$, 0.2, and 0.3, respectively. With our diamond ATR crystal ($\Theta_i = 45°$), the penetration depth at 1000 cm^{-1} decreased from 1.679 μm at $x = 0$ to 1.661 μm at $x = 0.3$, a variation that affected the intensities by less than 1.2%. A much more serious problem arose from the relatively low refractive index of the diamond, which caused marked distortions of the intense absorptions in the 1100−1300 cm^{-1} region. However, we checked that absorptions of moderate or low intensity had the same profile in the ATR and transmission experiments, and we used the ATR spectra only for such bands.

CHART 1: Stable Complexes Obtained from DFT B3LYP/6-31G Calculations, with Respective Symmetries Indicated in Brackets**

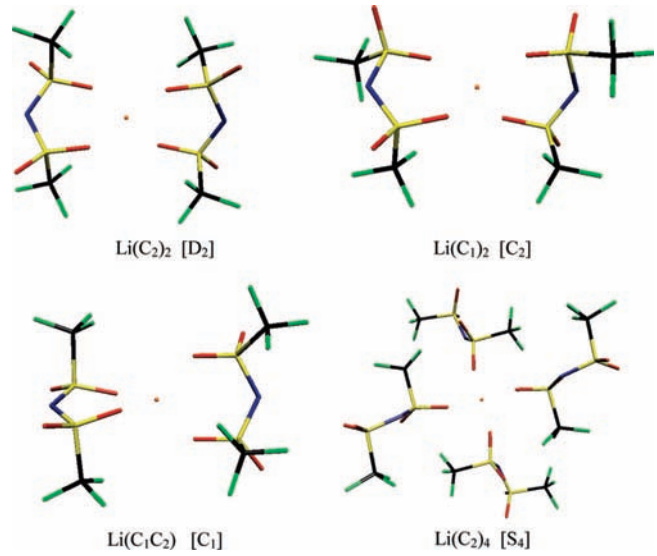

The DFT calculations were performed on three different $[Li(TFSI)_2]^-$ complexes, based on the lithium ion being doubly bidentately coordinated by two $TFSI^-$ anions adopting the same C_2 or C_1 conformation, denoted as $Li(C_2)_2$ or $Li(C_1)_2$, respectively, or a mixed conformation complex, denoted as $Li(C_2C_1)$ (Chart 1). In addition, a $[Li(TFSI)_4]^{3-}$ complex was constructed with all $TFSI^-$ anions in the C_2 conformation, resulting in a total S_4-symmetry complex, denoted as $Li(C_2)_4$ (Chart 1). Geometry optimizations and subsequent frequency calculations were performed using Becke's three-parameter hybrid method with the Lee−Yang−Parr correlation functional (B3LYP).[17−19] The Pople type basis set 6-31G** was chosen, as the B3LYP/6-31G** combination has been shown to provide realistic molecular geometries and vibrational frequencies for the free $TFSI^-$ anion.[20] In addition, a larger Pople basis set was also used (6-311+G*). All calculations were performed using the Gaussian 03 program package.[21]

For the comparison between the calculated and experimental spectra, we report either the directly calculated lines for the free C_2 and C_1 conformers of $TFSI^-$ or a convolution of these calculated lines by a Gaussian function in the case of the complexes. Indeed, the complexes exhibit a large number of lines, sometimes superimposed and it is more convenient and instructive to visualize their convoluted spectra.

TABLE 2: Selected Geometry Data and Energies for the Three Complexes Li(C_2)$_2$, Li(C_1)$_2$, and Li(C_2C_1) Obtained Using the B3LYP Functional and the 6-31G and 6-311+G* Basis Sets**

	Li(C_2)$_2$		Li(C_1)$_2$		Li(C_2C_1)	
	6-31G**	6-311+G*	6-31G**	6-311+G*	6-31G**	6-311+G*
Li—O (Å)	1.945	1.946	1.950, 1.962	1.946, 1.955	1.950−1.958	1.944−1.949
S—N (Å)	1.615	1.605	1.610, 1.616	1.603, 1.607	1.610−1.616	1.603−1.607
S—O[a] (Å)	1.486	1.477	1.485, 1.486	1.477, 1.478	1.485−1.487	1.477−1.478
S—O (Å)	1.459	1.452	1.456, 1.460	1.451, 1.453	1.458−1.460	1.451−453
S—N—S (deg)	123.7	125.8	124.5	126.1	123.7, 124.5	125.9, 126.2
C—S—N—S (deg)	94.3	102.6	85.6	99.2	94.1, 86.8	101.9, 99.6
C—S—N—S (deg)	94.3	102.6	−116.4	−119.9	94.5, −118.2	103.9, −119.1
E [au]		−3662.80586		−3662.80140		−3662.80363
ΔH [kJ mol^{-1}]		0		+11.6		+5.9
ΔE_{bind} [kJ mol^{-1}]		−788.0		−776.3		−782.2

[a] Coordinated by Li.

Results and Discussion

The results of the DFT calculations are first briefly summarized; then, some specific IR and Raman bands are carefully analyzed with the help of the calculated spectra to determine the conformation of the coordinated anions and the vibrations of the lithium ion inside its solvating cage. Finally, the quantitative approach used to determine the lithium ion solvation number is critically investigated.

1. DFT Calculations. Our calculations on the isolated TFSI$^-$ anion (Table S1)[20] and on the three [Li(TFSI)$_2$]$^-$ complexes (Table S2) are in good agreement with those reported by Fujii et al.[22] and by Umebayashi et al.,[10] respectively. However, there are some differences in the interpretation of the usefulness of various computational approaches and thus the resulting data. In Table 2, selected geometric data and energies are reported for the three complexes as obtained using the B3LYP functional and both the 6-31G** and 6-311+G* basis sets. In general, very small differences were found between the complexes, in agreement with ref 10, as well as between the different basis sets used. The most noticeable differences are the shortening of the S—O bonds (i.e., more double-bond character) and the widening of some of the dihedrals of the Li(C_1)$_2$ and Li(C_2C_1) complexes for the 6-311+G* basis set, but almost complete insensitivity of the S—N—S angles to the type of complex and their total additivity, i.e., unchanged due to the different couplings through the Li. For the energies, we found the Li(C_2)$_2$ complex to be rather more stable than the others, with each C_1 conformer in the complexes adding about 5.8−6.9 kJ mol^{-1} to the enthalpy (H). Even though we used the same method as Umebayashi et al.,[10] we obtained significantly larger energetic differences between the complexes and, in addition, the opposite trend for the lithium ion binding energies [we found Li(C_2)$_2$ > Li(C_2C_1) > Li(C_1)$_2$]. The latter might be due to a different choice of reference for these calculations (we used the most stable conformer, C_2, of free TFSI$^-$ as the reference, whereas in ref 10, the choice is unclear). The former might be due to the difference between the use of electronic energies and enthalpies, but there are also small notable geometry differences.

Because [Li(TFSI)$_n$]$^{(n-1)-}$ complexes with $n = 3$ and 4[4,12,14] have also been postulated, we report in Table S3 the calculated spectra of Li(C_2)$_4$. For the computational generation of IR and Raman spectra, we acknowledge, in agreement with Umebayashi et al.,[10] that the 6-311+G* basis set gives the best overall spectral agreement. In contrast, however, we still prefer to use the 6-31G** basis set results, as they significantly better reproduce the details of the frequency shifts of the important vibrations in the regions of particular interest. We believe this to be one crucial key to a more unambiguous interpretation of the spectra of the complexes, and this is shown below, where all spectral computational results are those of the B3LYP/6-31G** method.

2. Vibrational Assignments and Conformation of the Coordinated Anions. ***2.1. General Considerations.*** In previous studies of LiTFSI solutions and LiTFSI-doped ILs using IR and Raman spectroscopies, some vibrational modes of the TFSI$^-$ anion have already been identified as suitable probes for the lithium ion coordination.[20,23−27] Let us recall however that, even in the absence of lithium, a given TFSI$^-$ vibration might undergo frequency shifts, depending on the nature of the surrounding solvent, and there might also be frequency splits due to the presence of two TFSI$^-$ conformers. The conformational equilibrium between the trans (C_2) and cis (C_1) forms of the TFSI$^-$ anion was indeed theoretically predicted ca. 10 years ago[28] and more recently experimentally verified by the IR and Raman spectra of various LiTFSI solvates involving solvent-separated ion pairs (SSIPs)[20] in the Et$_4$NTFSI melted and disordered phases[29] and in the solid and liquid phases of EMITFSI.[22,30] Initially, the isolated C_2 conformer of gaseous TFSI$^-$ was calculated by ab initio methods to be more stable than the C_1 conformer by about 2.3 kJ mol^{-1}. This energy difference was found to be 2.2 kJ mol^{-1} for diluted solutions of LiTFSI in aprotic solvents,[20] 3.5 or 4.5 kJ mol^{-1} for liquid EMITFSI,[22,30] and 7 kJ mol^{-1} for the Et$_4$NTFSI disordered phase (322−317 K).[29] The conformational state of the coordinated TFSI$^-$ anion is less well-known. Preliminary Raman results simply indicate a tendency of the anion to adopt the C_1 (cis) conformation upon lithium coordination,[5,10] and the crystal structure of the Li$_2$(EMI)(TFSI)$_3$ compound reveals that two anions have a cis conformation and the third a trans conformation.[6]

Altogether, it is necessary to keep in mind the possibility of non-negligible conformational and solvent effects when analyzing the effects of the lithium ion coordination on the vibrational spectra, especially as their respective magnitudes might vary from one TFSI$^-$ vibrational mode to the other. In the following vibrational analysis, we have tried to take all of these contributions into account for an unambiguous identification of the perturbations specifically due to lithium ion coordination. Of course, the anion vibrations, and thus also the complexes, can be analyzed only in spectral regions where they are not obscured by contributions of the imidazolium derivative, which can be determined through a comparison of the IR and Raman spectra of EMITFSI and EMIBr (Figure S1).

2.2. Spectral Range 1400−800 cm^{-1}. Because Li$^+$ interacts essentially with the sulfonyl oxygen atoms of TFSI$^-$, the stretching vibrations of the SO$_2$ groups are obvious candidates to reveal this interaction in LiTFSI-doped ILs. However, each

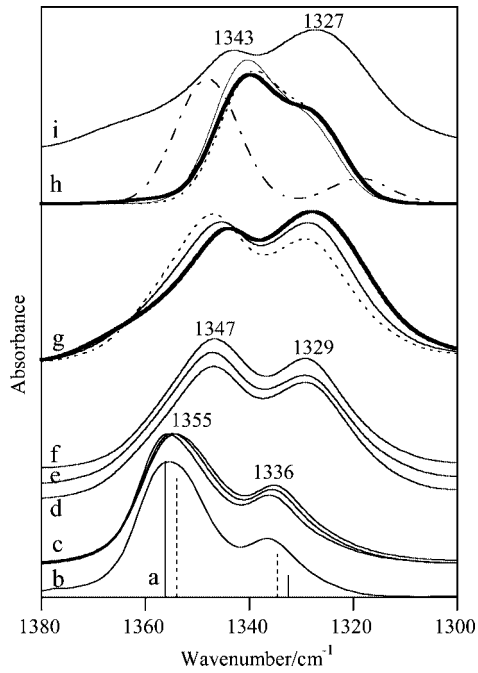

Figure 1. (a) Calculated IR spectra of the C_2 (vertical solid line) and C_1 (vertical dotted line) conformers of $TFSI^-$ in the region of the $\nu_a{}^{ip}SO_2$ and $\nu_a{}^{op}SO_2$ vibrations. Experimental ATR-FTIR spectra of (b) EMITFSI solution in diglyme; (c) EMITFSI solution in acetonitrile for molar ratios of 1/100, 1/50, and 1/30 by order of increasing intensity at 1336 cm^{-1}; the pure ionic liquids (d) EMITFSI, (e) BMITFSI, and (f) BMMITFSI; and (g) $(1 - x)$BMITFSI,xLiTFSI for $x = 0$ (dotted line), 0.18 (thin line), and 0.37 (heavy line). (h) Calculated IR spectra of the complexes $Li(C_2)_2$ (thin line), $Li(C_1)_2$ (dotted line), $Li(C_2C_1)$ (heavy line), and $Li(C_2)_4$ (dot-dashed line). (i) Experimental IR spectrum of the $x = 0.37$ doped sample after subtraction of the contribution of the spectrum of pure BMITFSI (see text). All calculated wavenumbers were scaled by a multiplicative factor of 1.025. The calculated intensities in h were convoluted by a Gaussian function with a fwhm of 13 cm^{-1}.

$TFSI^-$ anion holds two SO_2 groups that do not vibrate independently. This produces a splitting of each SO_2 vibrational mode into in-phase and out-of-phase components.[23] In addition, when several $TFSI^-$ anions are coordinated by a lithium ion, a further coupling can occur between the coordinated SO_2 groups. This coupling depends on the strength and structure of the complex. Thus, the antisymmetric stretching vibration, ν_aSO_2, typically situated in the 1300−1370 cm^{-1} region, and the symmetric stretching vibration, ν_sSO_2, situated in the 1100−1160 cm^{-1} region, could involve up to four components in a complex of the $[Li(TFSI)_2]^-$ type. This applies also to other vibrations of the SO_2 group such as the deformation mode δSO_2 situated in the 600−620 cm^{-1} region. The basic assignments of the $TFSI^-$ anion vibrational modes are taken from ref 23.

In Raman spectroscopy, the in-phase and out-of-phase antisymmetric stretching vibrations, $\nu_a{}^{ip}SO_2$ and $\nu_a{}^{op}SO_2$, respectively, have been observed for $TFSI^-$ solvated in various media at ∼1350 and 1330 cm^{-1}, respectively.[23,27] They are however completely hidden by intense lines due to the imidazolium derivatives of the ILs. In contrast and fortunately, the IR absorptions of the imidazolium derivatives in the 1380−1300 cm^{-1} range are negligibly weak compared to the ν_aSO_2 absorptions. The ATR-FTIR spectra of various EMITFSI solutions are reported in Figure 1b,c. Depending on the nature of the solvent, the $\nu_a{}^{ip}SO_2$ and $\nu_a{}^{op}SO_2$ modes are centered in the 1355−1352 and 1336−1330 cm^{-1} regions, respectively. These bands are fairly well reproduced by the calculated lines of the "free" anion (Figure 1a), although the conformational splitting of ca. 2 cm^{-1} between the C_2 and C_1 conformers cannot be resolved. It can be pointed out, however, that C_2 contributes more to the $\nu_a{}^{ip}SO_2$ component than C_1 and vice versa for the $\nu_a{}^{op}SO_2$ component. Therefore, as already argued, the effect of the temperature on a LiTFSI solution,[20] the relative increase of the $\nu_a{}^{op}SO_2$ intensity when the EMITFSI concentration in acetonitrile increases or when the polarity of the solvent increases can be interpreted by a shift of the conformational equilibrium toward the theoretically less stable C_1 conformer. Let us recall that the dipole moments are 5.42 and 0.67 D for the C_1 and C_2 conformers, respectively.[20] The spectra of the pure ILs are quite similar, indicating that the substitutions on the imidazolium ring have little effect on the profile of the $\nu_a{}^{ip}SO_2$ and $\nu_a{}^{op}SO_2$ components, now shifted to 1347 and 1329 cm^{-1}, respectively (Figure 1d−f). The variation of their relative intensity indicates a further displacement of the conformational equilibrium toward C_1. The C_1 population in EMITFSI at room temperature has previously been evaluated to be ∼25%.[30] The effect of the addition of LiTFSI to one of these ILs, BMITFSI, is illustrated in Figure 1g. The calculated spectra of the four model complexes are reported in Figure 1h. To approach the "true" experimental spectrum of the complex, supposed to have the $[Li(TFSI)_2]^-$ stoichiometry, a difference spectrum is given in Figure 1i. It was obtained by subtracting a fraction of the spectrum of pure BMITFSI corresponding roughly to the amount of uncoordinated anions remaining in the doped sample ($1 - 2x \approx 26\%$), from the spectrum of the $x = 0.37$ doped sample. Subtraction spectra were also used in several other spectral regions. In cases where separate bands of the "free" and "coordinated" species were observed, it appears that the free components are satisfactorily canceled. This method is not intended to provide accurate quantitative measurements, but to facilitate the visual comparison with the calculated spectra of the complexes. In the subtraction spectrum of Figure 1i, the $\nu_a{}^{ip}SO_2$ and $\nu_a{}^{op}SO_2$ components are seen to be shifted to 1343 and 1327 cm^{-1}, respectively, and their relative intensity is still modified in favor of the latter. The calculated spectrum of $Li(C_2)_4$ strongly disagrees with both the experimental positions and intensities, whereas the calculated spectra of the $Li(C_1)_2$, $Li(C_2)_2$, and $Li(C_2C_1)$ complexes are very similar and reproduce the observed frequency shift to lower wavenumbers, although the intensities are less well reproduced. At this stage, it is not possible to choose between the $Li(C_1)_2$, $Li(C_2)_2$, and $Li(C_2C_1)$ models.

As the next step, the in-phase and out-of-phase symmetric stretching vibrations, $\nu_s{}^{ip}SO_2$ and $\nu_s{}^{op}SO_2$, respectively, can be observed in the IR spectra of the three ILs (Figure 2b−d). The main maximum at 1132 cm^{-1} corresponds to the $\nu_s{}^{ip}SO_2$ mode, with a predominant contribution of the C_2 conformer, and the shoulder at 1143 cm^{-1} comes from the $\nu_s{}^{op}SO_2$ component of the C_1 conformer (Figure 2a). Addition of LiTFSI causes a small shift of the $\nu_s{}^{ip}SO_2$ mode to lower wavenumbers (Figure 2e). The spectrum of the complex (Figure 2g) was obtained by subtraction as previously described for ν_aSO_2. The four calculated spectra are now very different, and the best agreement with the experimental profile is observed for the $Li(C_2C_1)$ complex (with a minor change in the scaling factor from 1.018 in Figure 1a to 1.037 in Figure 1f). The same kind of observations can be made for the Raman spectra of the $\nu_s{}^{ip}SO_2$ and $\nu_s{}^{op}SO_2$ modes of the three ILs (Figure 3a−d), but the calculated spectra of the four complexes are now similar (Figure 3f) and there is only a slightly better agreement of the $Li(C_2C_1)$ spectrum with the experimental profile (Figure 3g).

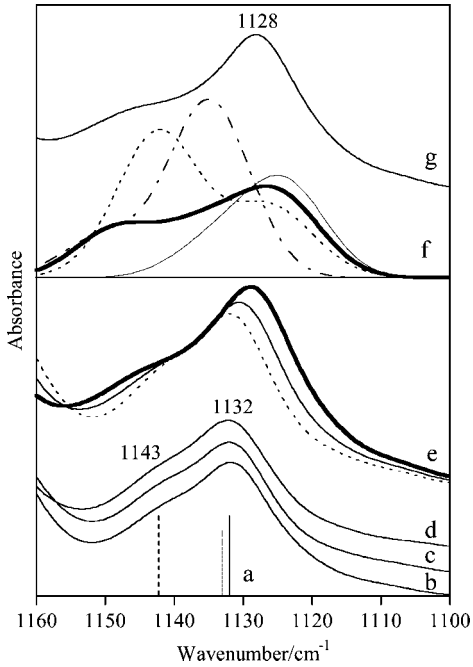

Figure 2. (a) Calculated IR spectra of the C_2 (vertical solid line) and C_1 (vertical dotted line) conformers of $TFSI^-$ in the region of the $\nu_s^{ip}SO_2$ and $\nu_s^{op}SO_2$ vibrations. Experimental ATR-FTIR spectra of (b) EMITFSI; (c) BMITFSI; (d) BMMITFSI; and (e) $(1-x)$BMITFSI,xLiTFSI ionic liquids with $x = 0$ (dotted line), 0.18 (thin line), and 0.37 (thick solid line). (f) Calculated IR spectra of the complexes $Li(C_2)_2$ (thin line), $Li(C_1)_2$ (dotted line), $Li(C_2C_1)$ (heavy line), and $Li(C_2)_4$ (dot-dashed line). (g) Experimental IR spectrum of the $x = 0.37$ doped sample after subtraction of the contribution of the spectrum of pure BMITFSI (see text). The calculated wavenumbers were scaled by a multiplicative factor of 1.018 in a and by a factor of 1.037 in f. The calculated intensities in f were convoluted by a Gaussian function with a fwhm of 13 cm^{-1}.

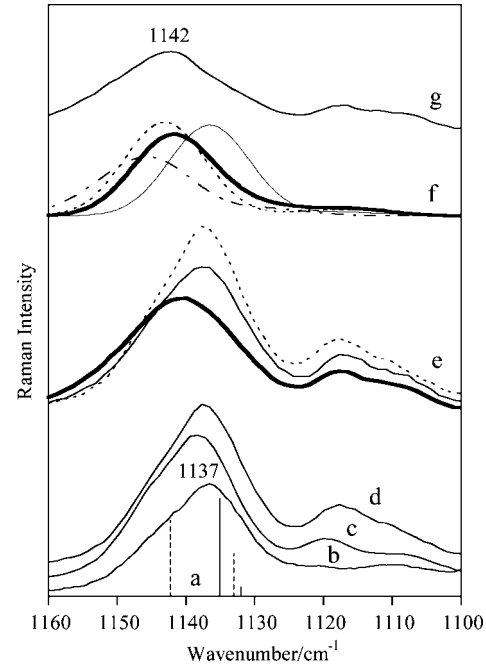

Figure 3. (a) Calculated Raman spectra of the C_2 (vertical solid line) and C_1 (vertical dotted line) conformers of $TFSI^-$ in the region of the $\nu_s^{ip}SO_2$ and $\nu_s^{op}SO_2$ vibrations. Experimental spectra of (b) EMITFSI; (c) BMITFSI; (d) BMMITFSI; and (e) $(1-x)$BMITFSI,xLiTFSI ionic liquids with $x = 0$ (dotted line), 0.18 (thin line), and 0.37 (thick solid line). (f) Calculated Raman spectra of the complexes $Li(C_2)_2$ (thin line), $Li(C_1)_2$ (dotted line), $Li(C_2C_1)$ (heavy line), and $Li(C_2)_4$ (dot-dashed line). (g) Experimental Raman spectrum of the $x = 0.37$ doped sample after subtraction of the contribution of the spectrum of pure BMITFSI (see text). The calculated wavenumbers were scaled by a multiplicative factor of 1.018 in a and by a factor of 1.031 in f. The calculated intensities in f were convoluted by a Gaussian function with a fwhm of 13 cm^{-1}.

In the region between the ν_aSO_2 and ν_sSO_2 modes, both the IR and Raman spectra exhibit very intense bands due to the ν_aCF_3 and ν_sCF_3 vibrations. There is also an intense IR absorption at 1060 cm^{-1} assigned to the ν_aSNS vibration.[23] Addition of LiTFSI to the pure ILs produces only small changes in the profiles of these bands.

2.3. Spectral Range 700−500 cm^{-1}. The 680−480 cm^{-1} spectral range has previously been shown to contain separated IR bands of the two $TFSI^-$ conformers for LiTFSI dissolved in solvents or polymers.[20] This is also true for the three pure ILs for which the IR spectra (Figure 4b−d) are very similar to those obtained for LiTFSI dissolved in various solvents (Figure 5 of ref 20). The cation absorptions are negligibly weak in this region. Small differences between the three ILs appear only near 650−660 cm^{-1} because of a contribution of $BMMI^+$. The comparison with the calculated spectra shows that the band at 618 cm^{-1} is due only to the C_2 conformer whereas the bands at 651 and 601 cm^{-1} are due only to the C_1 conformer. The well-separated bands at 571 and 515 cm^{-1} are both due to mixed contributions of the two conformers. The vibrational assignment of several of these absorptions have already been discussed in terms of deformation modes of the SNS, OSO and CF_3 groups.[20] Addition of LiTFSI very slightly modifies the relative intensities of the bands now centered at 615 and 658 cm^{-1}, but produces a clear decrease of the 571 cm^{-1} band, associated with the concomitant increase of a new band at 581 cm^{-1} (Figure 4e). Another couple of bands at 515/522 cm^{-1} reveals the equilibrium between free and coordinated anions. The calculated spectrum of the $Li(C_2)_4$ complex differs markedly from the subtraction spectrum of Figure 4g. Those of the $Li(C_2)_2$ and $Li(C_1)_2$ complexes are also different: the former does not reproduce the 658 cm^{-1} component, and the latter does not reproduce the 615 cm^{-1} one. Only the $Li(C_2C_1)$ complex gives an acceptable agreement with the experimental profile.

2.4. Spectral Range 500−200 cm^{-1}. Let us first consider the far-IR spectra reported in Figure 5b,c. It has already been established that the vibrations of the lithium ion in its coordinating cage, also called "rattling" motions, produce absorptions in the 500−300 cm^{-1} region.[27,31−33] Liquid EMITFSI exhibits several bands at ∼409, 362, and 287 cm^{-1} that are well reproduced by the calculation of the free conformers of $TFSI^-$ (Figure 5a). Progressive addition of LiTFSI is accompanied by the proportional increase of a broad absorption centered at 374 cm^{-1}. The calculated lines in this region for the model complexes correspond well to large-amplitude lithium motions. This is illustrated in Figure 6 for the $Li(C_2C_1)$ complex. The resulting Li^+ rattling motions characterize the short-time dynamics of the lithium ion within its solvating cage. The rather high wavenumber of the main band means that the Li^+ coordination is relatively strong and the complex long-lived, in agreement with the idea that the lithium diffusion in LiTFSI-doped ILs partly occurs through diffusion of a $Li(TFSI)_2$ complex.[13] It is obvious from Figure 5 that the transitions due to the Li^+ vibrations are more broadened than those of any internal mode of the anion. This is not surprising in view of the marked anharmonic character of the lithium ion motions. It follows that no differentiation can be made between the three $Li(TFSI)_2$ complexes in this IR spectral range (Figure 5d). The

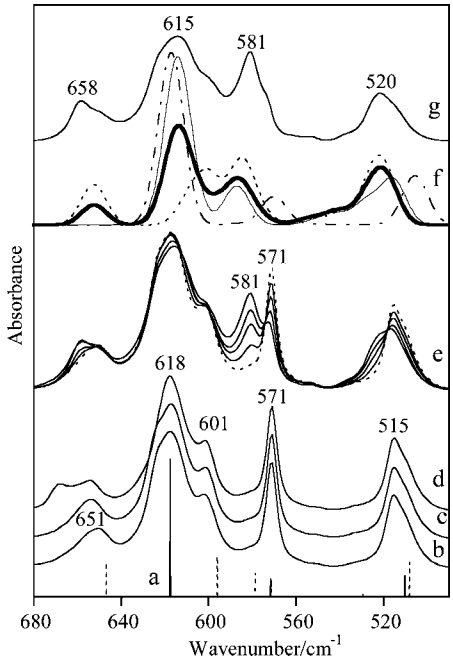

Figure 4. (a) Calculated IR spectra of the C_2 (vertical solid lines) and C_1 (vertical dotted lines) conformers of $TFSI^-$. Experimental IR spectra, recorded in transmission between two CsI windows, of (b) EMITFSI; (c) BMITFSI; (d) BMMITFSI; and (e) $(1 - x)$EMITFSI,xLiTFSI for $x = 0$ (dotted line), 0.1, 0.2, 0.3, and 0.4 by order of decreasing intensity at 581 cm^{-1} and of increasing intensity at 571 cm^{-1}. (f) Calculated IR spectra of the complexes $Li(C_2)_2$ (thin line), $Li(C_1)_2$ (dotted line), $Li(C_2C_1)$ (heavy line), and $Li(C_2)_4$ (dot-dashed line). (g) Experimental IR spectrum of the $x = 0.4$ doped sample after subtraction of the contribution of the spectrum of pure BMITFSI (see text). All calculated wavenumbers were scaled by a multiplicative factor of 1.025. The calculated intensities in f were convoluted by a Gaussian function with a fwhm of 13 cm^{-1}.

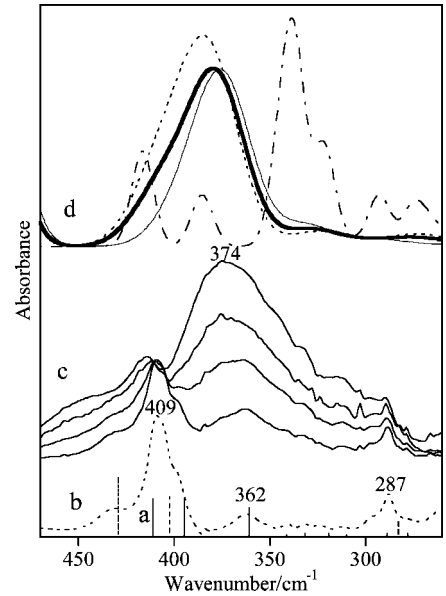

Figure 5. (a) Calculated IR spectra of the isolated $TFSI^-$ conformers of symmetry C_2 (vertical solid line) and C_1 (vertical dotted line). Experimental IR spectra, recorded in transmission between two CsI windows, of $(1 - x)$EMITFSI,xLiTFSI for (b) $x = 0$ (dotted line) and (c) $x = 0.1$, 0.2, 0.3, and 0.4 by order of increasing intensity at 374 cm^{-1}. (d) Calculated IR spectra of the complexes $Li(C_2)_2$ (thin line), $Li(C_1)_2$ (dotted line), $Li(C_2C_1)$ (heavy line), and $Li(C_2)_4$ (dot-dashed line). No scaling factor was applied to the calculated wavenumbers. The calculated intensities in d were convoluted by a Gaussian function with a fwhm of 33 cm^{-1}.

$Li(C_2)_4$ model again produces a spectrum very different from the experimental spectrum.

The Raman spectra of the EMITFSI, BMITFSI, and BMMITFSI ILs are very similar in the 450−250 cm^{-1} region because the contribution of the cations is negligibly weak (Figure S1). Earlier, some of us favored the 360−260 cm^{-1} region because of the presence of isolated lines of the C_2 and C_1 $TFSI^-$ conformations, for example, at 340 cm^{-1} (C_2) and 326 cm^{-1} (C_1).[30] Fujii et al. instead considered the couple of bands at 398 (C_2) and 407 cm^{-1} (C_1) (Figure 7a).[22] The two approaches do, however, lead to consistent values of the enthalpy of conformational change from C_2 to C_1: 4.5 or 3.5 kJ mol^{-1}.[22,30] DFT calculations for the Raman transitions of the two conformers were also performed.[22,30] The agreement with the experimental spectra is quite satisfactory once the presence of ∼75% C_2 conformers at room temperature is taken into account.

The interpretation of the spectral changes occurring after doping by LiTFSI is not as well-established. Based on a combination of Raman spectroscopy and DFT calculations, Umebayashi et al. suggested the formation of $[Li(TFSI)_2]^-$ ion clusters with a preference for the C_1 conformation for the coordinated anions,[10] a conclusion also reached by some of us.[5] In our present study, as seen in Figure 7b,c, the $Li(C_1)_2$ complex reproduces rather well most of the observed bands, including the asymmetric band at 326 cm^{-1}, but it does not reproduce the 312 cm^{-1} band at all. On the other hand, the $Li(C_2)_2$ complex reproduces well the 312 cm^{-1} band, but has no component at 326 cm^{-1}. The worst and best agreements are again obtained with the $Li(C_2)_4$ and $Li(C_2C_1)$ models, respectively.

In conclusion, the coordination of Li^+ by $TFSI^-$ anions leads to moderate but systematic perturbations of the anion vibrations. Some vibrations, such as the ν_aSO_2 and ν_sSO_2 stretching modes, directly related to lithium coordination, are less perturbed than expected. Some other vibrations, such as the 571 cm^{-1} IR absorption, involving the deformation of the SO_2 and CF_3 modes,[20] exhibit a clear transformation after coordination into a new absorption at 581 cm^{-1} (Figure 4). The DFT calculations allow these spectral changes to be predicted, provided that a good model of coordination of the lithium ion by the anions is selected. From the above analysis using four different model complexes, the $Li(C_2)_4$ model can clearly be excluded, and the best overall agreement can be confirmed for the $Li(C_2C_1)$ model. However, it must be pointed out that an equilibrium between equivalent quantities of the $Li(C_2)_2$ and $Li(C_1)_2$ complexes would give a comparable agreement as the $Li(C_2C_1)$ model. Indeed, the vibrational spectra of $Li(C_2C_1)$ are roughly a combination of those of $Li(C_2)_2$ and $Li(C_1)_2$. The $Li(C_2C_1)$ structure might then be considered as an intermediate structure between the other two.

Some comments can be added on the fact that interesting features of the ILs can be observed below 200 cm^{-1}. For several pure ILs, Fumino et al. reported the presence of an absorption band around 100 cm^{-1} due to cation−anion interionic vibrations.[34] Terahertz complex dielectric spectra in the 5−140 cm^{-1} domain have also been investigated in terms of interionic motions and of local structures.[35] Similarly, low-frequency Raman spectra (5−150 cm^{-1}) exhibit broad bands assigned to collective modes of local nanostructures.[36] Therefore, one can conclude that intraionic and interionic vibrations in ILs occur above and below ∼150 cm^{-1}, respectively.

3. Quantitative Approach and Lithium Coordination Number. ***3.1. Raman Spectral Range 800−700 cm^{-1}.*** The very intense Raman line situated at 740−750 cm^{-1}, due to an overall

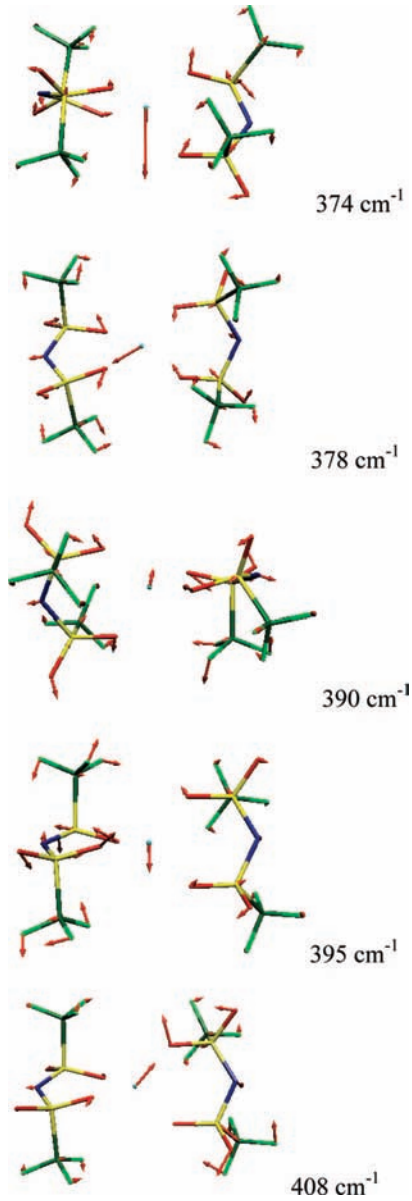

Figure 6. Calculated eigenvectors at the indicated wavenumbers for the Li(C_2C_1) complex.

anion expansion and contraction,[23] has very often been used to investigate the lithium solvation by $TFSI^-$.[1,5,7,10,12] When the anion is surrounded only by bulky alkyl-substituted imidazolium cations, it is situated at 740−744 cm^{-1}, i.e., at about the same position as observed for $TFSI^-$ solvated in various solvents or polymers.[20,23−25] The range 740−744 cm^{-1} illustrates the magnitude of the solvent effect experienced by the considered vibration of a pseudofree anion. Furthermore, this vibration has been shown to have a conformational splitting of 2−3 cm^{-1} in the gas state. This splitting is not resolved in the liquid state, so the conformational effect simply contributes to the broadening of the whole Raman profile centered at 740−744 cm^{-1}. The Raman spectra of three pure ILs are compared to the calculated lines of the C_2 and C_1 conformers in Figure 8. The ILs exhibit a very similar main band at ∼742 cm^{-1} having a full-width at half-maximum (fwhm) at room temperature of 6.7 cm^{-1}, resulting from the weighted contribution of the C_2 and C_1 conformers. This main band is accompanied by a much weaker band of the anion at about 765 cm^{-1} and by a band of the $BMMI^+$ cation near 725 cm^{-1}. As soon as a lithium ion is present in the first solvation shell of $TFSI^-$, a new line due to

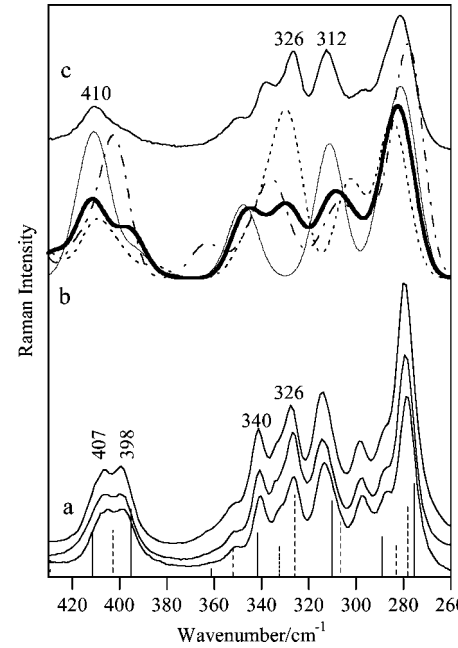

Figure 7. (a) Calculated Raman spectra of the isolated $TFSI^-$ conformers of symmetry C_2 (vertical solid line) and C_1 (vertical dotted line) and experimental Raman spectra of EMITFSI, BMITFSI, and BMMITFSI, from bottom to top. (b) Calculated Raman spectra of the complexes Li(C_2)$_2$ (thin line), Li(C_1)$_2$ (dotted line), Li(C_2C_1) (heavy line), and Li(C_2)$_4$ (dot-dashed line). (c) Experimental Raman spectrum of the (1 − x)EMITFSI,xLiTFSI mixture with x = 0.4. All calculated wavenumbers were multiplied by a scaling factor of 1.051, and the intensities in b were convoluted by a Gaussian function with a fwhm of 13 cm^{-1}.

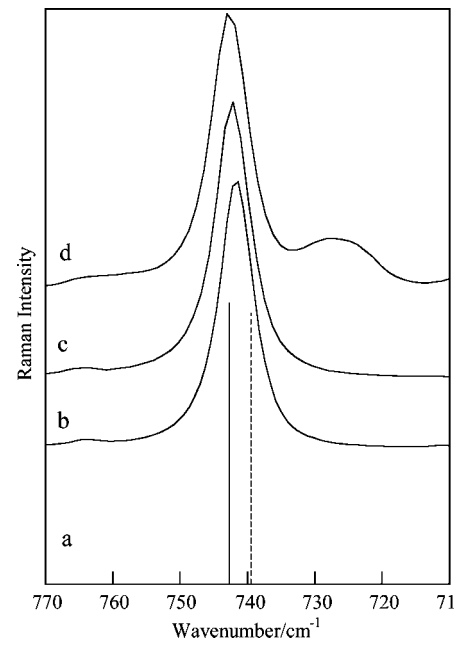

Figure 8. (a) Calculated Raman spectra of the isolated $TFSI^-$ conformers of symmetry C_2 (vertical solid line) and C_1 (vertical dotted line). Experimental Raman spectra of the pure ionic liquids (b) EMITFSI, (c) BMITFSI, and (d) BMMITFSI.

the formation of ion pairs can be resolved at 747−750 cm^{-1}. All previous spectroscopic analyses were performed by fitting the whole profile with only the two components at 740−744 and 747−750 cm^{-1}.[5,7,10,12,13] The Raman spectra of BMMITFSI doped with LiTFSI (Figure 9a) are very similar to those of EMITFSI or BMITFSI doped with LiTFSI.[5,7,10,12,13] They are

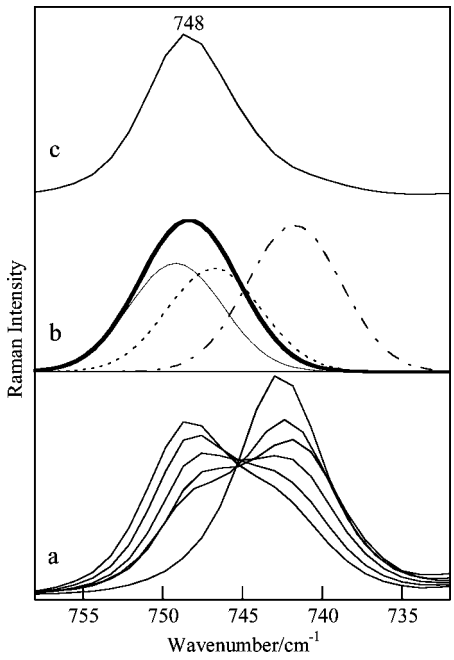

Figure 9. (a) Experimental Raman spectra of $(1 - x)$BMMITFSI,xLiTFSI with $x = 0$, 0.15, 0.2, 0.25, 0.3, and 0.35 by order of decreasing intensity at 742 cm^{-1} and increasing intensity at 748 cm^{-1}. (b) Calculated Raman spectra of the complexes $Li(C_2)_2$ (thin line), $Li(C_1)_2$ (dotted line), $Li(C_2C_1)$ (heavy line), and $Li(C_2)_4$ (dot-dashed line), after convolution by a Gaussian function with a fwhm of 7 cm^{-1}. (c) Experimental Raman spectrum of the $x = 0.35$ doped sample after subtraction of the contribution of the spectrum of pure BMMITFSI. The calculated wavenumbers were multiplied by a scaling factor of 1.037.

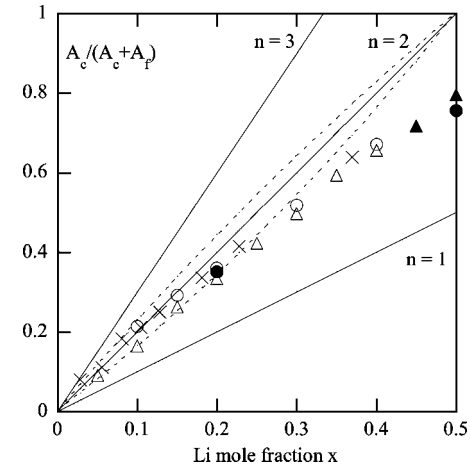

Figure 10. Plot of $A_c/(A_c + A_f)$ as a function of x for $(1 - x)$EMITFSI,xLiTFSI (circles), $(1 - x)$BMITFSI,xLiTFSI (crosses), and $(1 - x)$BMMITFSI,xLiTFSI (triangles). All data obtained at 298 K, except for the solid circles and triangles, which were obtained at 353 K. Solid lines corresponding to $n = 1$, 2, and 3 and $S = 1$ are shown for comparison. In the $n = 2$ case, the upper and lower dotted curves correspond to $S = 1.2$ and 0.8, respectively (see text).

also in agreement with the results reported by Monteiro et al.,[12] although these authors do not deduce any lithium coordination number from their Raman data. The calculated spectra in Figure 9b again illustrate the fact that the contribution of the $Li(C_2C_1)$ complex is roughly a combination of the contributions of the $Li(C_2)_2$ and $Li(C_1)_2$ complexes, whereas the band of the $Li(C_2)_4$ complex remains at the same position as that of the uncoordinated anion. The two calculated lines of $Li(C_2C_1)$, due to the coupling of the two anions, occur after scaling at 749.3 and 747.5 cm^{-1}. This splitting of about 2 cm^{-1} cannot be resolved in the liquid state. After convolution by a Gaussian function of with a fwhm of $\sim$7 cm^{-1}, the calculated profile is in good agreement with the subtraction spectrum of Figure 9c.

Under the hypothesis of the presence of only two components at 742 and 748 cm^{-1} in the spectra of Figure 9a, for example, two slightly different methods have been proposed in the literature to evaluate the lithium solvation number. Lassègues et al. assumed that the molar Raman scattering coefficients, s_{742} and s_{748}, were equal and normalized all of the spectra using the integrated intensity between 775 and 717 cm^{-1}.[5,13] This method was validated a posteriori by the presence of a pseudoisobestic point (see for example Figure 9a). Umebayashi et al. used an imidazolium band to normalize the spectra and also measured the decrease of the 742 cm^{-1} free component without making any hypothesis on the molar Raman scattering coefficients.[10] In this second method, the ratio s_{748}/s_{742} and the solvation number n were found equal to 0.9 and 1.86, respectively. The two methods led to consistent results, although the latter was applied to smaller LiTFSI dopings (Table 1).

For a quantitative evaluation of the solvation number n in the three investigated systems, we chose a method that differs slightly from the previous ones; it does not need any normalization of the spectra because it uses the intensity ratio $A_c/(A_c + A_f)$, where A_c and A_f are the integrated intensities of the 748 and 742 cm^{-1} components, respectively. If each lithium ion is assumed to be coordinated by n $TFSI^-$ anions, the concentration of these anions, which are responsible for the 748 cm^{-1} component, is given by $C_c = nxC_T$, where C_T is the total molar concentration of the $TFSI^-$ anions (see Table 1). It follows that $A_c = Ks_{748}nxC_T$, where K is a proportionality constant and s_{748} is the molar Raman scattering coefficient of the considered component. Similarly, the concentration of free $TFSI^-$ anions, which are responsible for the 742 cm^{-1} component, is $C_f = C_T - nxC_T$. Hence, $A_f = Ks_{742}(C_T - nxC_T)$. By setting $s_{748}/s_{742} = S$, it is easy to deduce that $A_c/(A_c + A_f) = Snx/(Snx - nx + 1)$. In the $S = 1$ limiting case,[5,13] the $A_c/(A_c + A_f) = f(x)$ plot is linear with a slope that directly gives n. The present results, obtained for a large LiTFSI concentration range (Figure 10), show that the three investigated systems behave similarly. As expected, the alkyl substitutions on the imidazolium cation have a negligible influence on the anion coordination with Li^+. Note that a few samples were studied at 353 K to extend the liquid domain up to $x = 0.5$. The corresponding data points fall on the room-temperature mean curve within experimental errors, showing that the equilibrium between free and coordinated anions is only weakly affected. The $n = 2$ straight line reproduces the experimental points much better than the $n = 1$ or $n = 3$ lines. Let us recall, however, that Umebayashi et al. found $S = 0.9$,[10] whereas a value of 1.2 can be deduced from the calculated data reported in Tables S1 and S2. The theoretical value has to be taken with care, but we tried to see how the uncertainty in S affects the evaluation of the solvation number by reporting in Figure 10 the curves obtained for $n = 2$ and $S = 1 \pm 0.2$. It appears that the differences between the two curves and the $n = 2$ straight line are of the same order of magnitude as the scattering of the experimental points at low concentration. In other words, a moderate fluctuation of S does not change the conclusion that the data up to at least $x = 0.2$ can be interpreted with a solvation number of 2. For higher doping levels, n becomes clearly smaller than 2.

One possible weakness of all of the previous methods is the use of only two components. Indeed, we saw that, in principle, the 742 cm^{-1} band contains the contribution of the two $TFSI^-$

free conformers and that the 748 cm^{-1} band comes essentially from a $[Li(TFSI)_2]^-$ complex of the $Li(C_2C_1)$ type that also involves two components. In each case, splittings of 2−3 cm^{-1} are predicted. Therefore, the whole profile should be fitted by four components instead of two. The challenge is to know whether four components can be reasonably fitted into the observed profiles. The comparison reported in Figure S2 shows that the agreement between the calculated and experimental profiles is not much better with four than with two components. In addition, even though the profile of each component is kept constant (40% Gaussian, 60% Lorentzian), the number of adjustable parameters remains high in the case of four components. Actually, the imprecision is much higher for the intensities than for the positions, as a small shift in the positions leads to large variations in the relative intensities. The fitted positions of the four components were found to vary continuously as a function of the concentration with the two doublets split by about 2 cm^{-1}, in good agreement with the DFT calculations (Figure S3), but the intensity results (not shown) are not accurate enough to be exploited. They simply indicate a qualitative agreement with the variation observed in Figure 10: the slope at high concentration ($x \geq 0.2$) gives more free anions than expected for an $n = 2$ stoichiometry. This result can hardly be reconciled with the existence of $[Li(TFSI)_n]^{(n-1)-}$ solvates with $n = 3$[9] or 4.[14] It is rather in favor of $[Li_m(TFSI)_n]^{(n-m)-}$ solvates, with $n/m < 2$, resulting from lithium aggregation, as suggested by Borodin et al.[4] However, we reach here the present limits of the Raman analysis because we still do not know if/how $[Li_m(TFSI)_n]^{(n-m)-}$ solvates can be spectroscopically differentiated from the simpler $[Li(TFSI)_2]^-$ complexes.

3.2. IR Spectral Range 800−700 cm^{-1}. The IR spectra (Figure 11) present strong similarities with the Raman ones, although they are much less intense. In fact, the coordination of $TFSI^-$ anions by alkali earth cations was first investigated using IR absorptions in the 710−770 cm^{-1} region by Bakker et al.[26] In the present study, the IR spectra of the three ILs all exhibit a main band at 740 cm^{-1}, accompanied by a weaker band at 762 cm^{-1}. The 740 cm^{-1} absorption certainly comes from the complex $TFSI^-$ mode responsible for the very intense Raman line at 740−742 cm^{-1}.[23] The calculated IR spectra exhibit only two bands at 716.1 and 713.1 cm^{-1} for the C_2 and C_1 conformers, respectively (Table S1).[20] After scaling, they produce the unresolved band observed at 740 cm^{-1} (Figure 11a). The 762 cm^{-1} absorption, observed in the three ILs (Figure 11b−d), as well as in quite different TFSI derivatives by Bakker et al.,[26] is due to a mode of strongly mixed C−F, S−N, and C−S stretchings.[23] However, it is not well reproduced in the calculated spectra. Note also that the EMI^+ cation presents a broad absorption centered at 754 cm^{-1} (Figure S1a), which explains the submaximum observed between the 740 and 762 cm^{-1} components for the EMI^+- (and BMI^+-) based ILs (Figure 11b).

Addition of LiTFSI to BMITFSI produces the series of spectra reported in Figure 11e. The subtraction spectrum in Figure 11g is very similar to those presented by Bakker et al., except for the supplementary band at 753 cm^{-1} discussed above. The 740 and 746 cm^{-1} bands were assigned by Bakker et al. to the S−N stretching modes of free and coordinated anions, respectively.[26] Even if the vibrational assignment in terms of group vibrations is somewhat ambiguous, these bands obviously behave as the 742/748 cm^{-1} couple of Raman lines. The intensity decrease of the 740 cm^{-1} band and the parallel increase of the ∼746 cm^{-1} band upon LiTFSI doping reflect the lithium ion coordination process. A quantitative analysis would, however, be much less accurate than for Raman spectroscopy and would not provide new information. The main absorption of the complex at ∼746 cm^{-1} is reproduced by the three computational DFT models, although with a much weaker intensity for $Li(C_2)_2$ than for $Li(C_1)_2$.

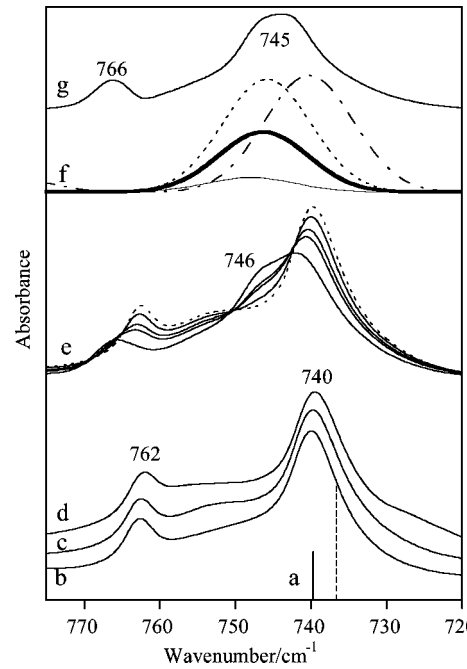

Figure 11. (a) Calculated IR spectra of the C_2 (vertical solid line) and C_1 (vertical dotted line) conformers of $TFSI^-$. Experimental ATR-FTIR spectra of (b) EMITFSI; (c) BMITFSI; (d) BMMITFSI; and (e) $(1 - x)$BMITFSI,xLiTFSI for $x = 0$, 0.08, 0.18, 0.227, and 0.37, by order of decreasing intensity at 740 and 762 cm^{-1} and increasing intensity at 746 cm^{-1}. (f) Calculated IR spectra of the complexes $Li(C_2)_2$ (thin line), $Li(C_1)_2$ (dotted line), $Li(C_2C_1)$ (heavy line), and $Li(C_2)_4$ (dot-dashed line). (g) Experimental IR spectrum of the $x = 0.37$ doped sample after subtraction of the contribution of the spectrum of pure BMITFSI (see text). All calculated wavenumbers were multiplied by a scaling factor of 1.037. The calculated intensities in f were convoluted by a Gaussian function with a fwhm of 13 cm^{-1}.

Conclusions

A systematic study of the IR and Raman spectra of the EMITFSI, BMITFSI, and BMMITFSI ionic liquids, before and after doping by LiTFSI, shows that, at low to medium LiTFSI concentration ($0.08 < x < 0.2$), a $[Li(TFSI)_4]^{3-}$ complex clearly can be excluded whereas the presence of a $[Li(TFSI)_2]^-$ complex is confirmed. Thanks to a detailed analysis of several vibrational modes of the anion and the support of DFT calculations of IR and Raman spectra, the anions in the $[Li(TFSI)_2]^-$ complex are shown to adopt a mixed C_2C_1 conformation. Yet another possibility, though unlikely, is a mixture of the pure complexes $Li(C_2)_2$ and $Li(C_1)_2$, but the mixed complex $Li(C_1C_2)$, by necessity, almost must be an intermediate and thus again the main track. To the best of our knowledge, the IR-active vibrations of the lithium ion inside its solvating cage have been evidenced for the first time in LiTFSI-doped ILs.

At higher concentration ($x \geq 0.2$), the mixed complex seems to be gradually replaced by other species where Li^+ is coordinated by less than two anions. As predicted by MD simulations,[4] $[Li_m(TFSI)_n]^{(n-m)-}$ aggregates with $n = 2m - 1$ could be formed, opening the way to a nanostructuring of the LiTFSI-doped ILs. However, our critical analysis of the potentialities and limitations of the IR and Raman spectroscopies

suggests that these aggregates would be difficult to identify spectroscopically.

Acknowledgment. The authors are grateful to D. Talaga and J.-L. Bruneel for their help in recording the Raman spectra. The Swedish Research Council (VR) and Stiftelsen Futura are thankfully acknowledged for research funding. We are also grateful to the Swedish National Infrastructure for Computing (SNIC) for granting computational resources.

Supporting Information Available: Observed IR and Raman spectra of EMIBr in CD_3CN solution and of pure EMITFSI (Figure S1). Examples of fits of the 740 cm^{-1} Raman band with two or four components (Figure S2) and fitted positions of these components (Figure S3). Calculated wavenumbers and intensities of the Raman and IR transitions of the free $TFSI^-$ conformers (Table S1); of the $Li(C_2)_2$, $Li(C_1)_2$, and $Li(C_1C_2)$ complexes (Table S2); and of $Li(C_2)_4$ (Table S3). This material is available free of charge via the Internet at http://pubs.acs.org.

References and Notes

(1) Castriota, M.; Caruso, T.; Agostino, R. G.; Cazzanelli, E.; Henderson, W. A.; Passerini, S. *J. Phys. Chem. A* **2005**, *109*, 92.
(2) Lee, S.-Y.; Yong, H. H.; Lee, Y. J.; Kim, S. K.; Ahn, S. *J. Phys. Chem. B* **2005**, *109*, 13663.
(3) Nicotera, I.; Oliviero, C.; Henderson, W. A.; Appetecchi, G. B.; Passerini, S. *J. Phys. Chem. B* **2005**, *109*, 22814.
(4) Borodin, O.; Smith, G. D.; Henderson, W. A. *J. Phys. Chem. B* **2006**, *110*, 16879.
(5) Lassègues, J. C.; Grondin, J.; Talaga, D. *Phys. Chem. Chem. Phys.* **2006**, *8*, 5629.
(6) Matsumoto, K.; Hagiwara, R.; Tamada, O. *Solid State Sci.* **2006**, *8*, 1103.
(7) Hardwick, L. J.; Holzapfel, M.; Wokaun, A.; Novák, P. *J. Raman Spectrosc.* **2007**, *8*, 5629.
(8) Ye, C.; Shreeve, J. M. *J. Phys. Chem. B* **2007**, *111*, 1456.
(9) Saito, Y.; Umecky, T.; Niwa, J.; Sakai, T.; Maeda, S. *J. Phys. Chem. B* **2007**, *111*, 11794.
(10) Umebayashi, Y.; Mitsugi, T.; Fukuda, S.; Fujimori, T.; Fujii, K.; Kanzaki, R.; Takeuchi, M.; Ishiguro, S.-i. *J. Phys. Chem. B* **2007**, *111*, 13028.
(11) Hayamizu, K.; Tsuzuki, S.; Seki, S.; Ohno, Y.; Miyashiro, H.; Kobayashi, Y. *J. Phys. Chem. B* **2008**, *112*, 1189.
(12) Monteiro, M. J.; Bazito, F. F.; Siqueira, L. J. A.; Ribeiro, M. C. C.; Torresi, R. M. *J. Phys. Chem. B* **2008**, *112*, 2102.
(13) Duluard, S.; Grondin, J.; Bruneel, J. L.; Pianet, I.; Grélard, A.; Campet, G.; Delville, M. H.; Lassègues, J. C. *J. Raman Spectrosc.* **2008**, *39*, 627.
(14) Umecky, T.; Saito, Y.; Okumura, Y.; Maeda, S.; Sakai, T. *J. Phys. Chem. B* **2008**, *112*, 3357.
(15) Henderson, W. A.; Brooks, N. R.; Young, V. G. *Chem. Mater.* **2003**, *15*, 4685.
(16) Gadjourova, Z.; Marero, D. M. y.; Andersen, K. H.; Andreev, Y. G.; Bruce, P. G. *Chem. Mater.* **2001**, *13*, 1282.
(17) Lee, C.; Yang, W.; Parr, R. G. *Phys. Rev. B* **1988**, *37*, 785.
(18) Becke, A. D. *J. Chem. Phys.* **1993**, *98*, 5648.
(19) Vosko, S. H.; Wilk, L.; Nusair, M. *Can. J. Phys.* **1980**, *58*, 1200.
(20) Herstedt, M.; Smirnov, M.; Johansson, P.; Chami, M.; Grondin, J.; Servant, L.; Lassègues, J. C. *J. Raman Spectrosc.* **2005**, *36*, 762.
(21) Frisch, M. J.; Trucks, G. W.; Schlegel, H. B.; Scuseria, G. E.; Robb, M. A.; Cheeseman, J. R.; Montgomery, J. A., Jr.; Vreven, T.; Kudin, K. N.; Burant, J. C.; Millam, J. M.; Iyengar, S. S.; Tomasi, J.; Barone, V.; Mennucci, B.; Cossi, M.; Scalmani, G.; Rega, N.; Petersson, G. A.; Nakatsuji, H.; Hada, M.; Ehara, M.; Toyota, K.; Fukuda, R.; Hasegawa, J.; Ishida, M.; Nakajima, T.; Honda, Y.; Kitao, O.; Nakai, H.; Klene, M.; Li, X.; Knox, J. E.; Hratchian, H. P.; Cross, J. B.; Bakken, V.; Adamo, C.; Jaramillo, J.; Gomperts, R.; Stratmann, R. E.; Yazyev, O.; Austin, A. J.; Cammi, R.; Pomelli, C.; Ochterski, J. W.; Ayala, P. Y.; Morokuma, K.; Voth, G. A.; Salvador, P.; Dannenberg, J. J.; Zakrzewski, V. G.; Dapprich, S.; Daniels, A. D.; Strain, M. C.; Farkas, O.; Malick, D. K.; Rabuck, A. D.; Raghavachari, K.; Foresman, J. B.; Ortiz, J. V.; Cui, Q.; Baboul, A. G.; Clifford, S.; Cioslowski, J.; Stefanov, B. B.; Liu, G.; Liashenko, A.; Piskorz, P.; Komaromi, I.; Martin, R. L.; Fox, D. J.; Keith, T.; Al-Laham, M. A.; Peng, C. Y.; Nanayakkara, A.; Challacombe, M.; Gill, P. M. W.; Johnson, B.; Chen, W.; Wong, M. W.; Gonzalez, C.; Pople, J. A. *Gaussian 03*, revision C.02; Gaussian, Inc.: Pittsburgh, PA, 2004.
(22) Fujii, K.; Fujimori, T.; Takamuku, T.; Kanzaki, R.; Umebayashi, Y.; Ishiguro, S.-i. *J. Phys. Chem. B* **2006**, *110*, 8179.
(23) Rey, I.; Johansson, P.; Lindgren, J.; Lassègues, J. C.; Grondin, J.; Servant, L. *J. Phys. Chem. A* **1998**, *102*, 3249.
(24) Edman, L. *J. Phys. Chem. B* **2000**, *104*, 7254.
(25) Brouillette, D.; Irish, D. E.; Taylor, N. J.; Perron, G.; Odziemkowski, M.; Desnoyers, J. E. *Phys. Chem. Chem. Phys.* **2002**, *4*, 6063.
(26) Bakker, A.; Gejji, S.; Lindgren, J.; Hermansson, K.; Probst, M. M. *Polymer* **1995**, *36*, 4371.
(27) Rey, I.; Lassègues, J. C.; Grondin, J.; Servant, L. *Electrochim. Acta* **1998**, *43*, 505.
(28) Johansson, P.; Gejji, S. P.; Tegenfeldt, J.; Lindgren, J. *Electrochim. Acta* **1998**, *43*, 1375.
(29) Herstedt, M.; Henderson, W. A.; Smirnov, M.; Ducasse, L.; Servant, L.; Talaga, D.; Lassègues, J. C. *J. Mol. Struct.* **2006**, *783*, 145.
(30) Lassègues, J. C.; Grondin, J.; Holomb, R.; Johansson, P. *J. Raman Spectrosc.* **2007**, *38*, 551.
(31) Chang, S.; Schmidt, P. P.; Severson, M. W. *J. Phys. Chem.* **1986**, *90*, 1046.
(32) Seneviratne, V.; Furneaux, J. E.; Frech, R. *Macromolecules* **2002**, *35*, 6392.
(33) Grondin, J.; Ducasse, L.; Bruneel, J. L.; Servant, L.; Lassègues, J. C. *Solid State Ionics* **2004**, *166*, 441.
(34) Fumino, K.; Wulf, A.; Ludwig, R. *Angew. Chem., Int. Ed.* **2008**, *47*, 3830.
(35) Yamamoto, K.; Tani, M.; Hangyo, M. *J. Phys. Chem. B* **2007**, *11*, 4854.
(36) Iwata, K.; Okajima, H.; Saha, S.; Hamaguchi, H.-O. *Acc. Chem. Res.* **2007**, *40*, 1174.

JP806124W